Lee *et al. Radiation Oncology* (2026) 21:73
https://doi.org/10.1186/s13014-026-02829-6

Radiation Oncology

RESEARCH Open Access

Machine learning approach to estimation of in vivo measured dose and treatment planning for total body irradiation

Sangmin Lee[1], Jung-in Kim[2,3,4,5], Seonghee Kang[2,3,4], Jaeman Son[2,3,4], Hyeongmin Jin[2,3,4], Chang Heon Choi[2,3,4,5], Jong Min Park[2,3,4,5], Joo Ho Lee[2,3,4,5], Ji Hyun Chang[2,3,4,5], Hyun-Cheol Kang[2,3,4,5] and Seongmoon Jung[6*]

Abstract

Purpose This study aims to enhance the conventional Total Body Irradiation (TBI) dose calculation method which relies on manual calculation using tissue maximum ratio, off axis ratio, and scatter factors, by incorporating machine learning (ML) to predict in vivo measured doses and optimize the number of compensators needed, thereby improving the accuracy and efficacy of TBI treatments.

Materials and methods A retrospective analysis was performed on patient data between 2018 and 2022, involving 96 patients. The data included demographics, treatment specifics, and in vivo dose measurements. We developed and evaluated various ML models, including Random Forest, XGBoost, LightGBM, and Gradient Boosting Regressor, using 70% of the data for training and 30% for testing. Model performance was assessed using the Mean Absolute Percentage Error (MAPE). The optimization process adjusted compensator numbers based on ML predictions to better align with the prescribed dose.

Results All ML models outperformed the conventional method, with Gradient Boosting Regressor demonstrating the best performance. It achieved an overall MAPE of 2.52% (maximum 2.95% at hip with hand, minimum 2.19% at umbilicus without arm) in predicting measured doses, which is a significant improvement compared to the conventional method's overall MAPE of 4.01% (maximum 8.69% at head, minimum 2.74% at umbilicus without arm). Furthermore, the optimization process successfully generated treatment plans with a high degree of conformity to the prescribed doses, achieving a MAPE of 1.69% between the optimized and prescribed doses. The head region, which exhibited the largest discrepancy in the conventional method, saw substantial improvement, while the neck region required an increase in compensators to correct underestimation.

Conclusion The machine learning approach successfully improved the accuracy of in vivo dose predictions and compensator optimization, suggesting an enhancement of conventional methods. This advancement holds the potential to deliver more precise and personalized radiation therapy in TBI treatments.

Keywords Total body irradiation, Machine learning, Dose prediction, Compensator optimization, In vivo dosimetry

*Correspondence:
Seongmoon Jung
smjung@kriss.re.kr

Full list of author information is available at the end of the article

Introduction

The total body irradiation (TBI) with MV photon beams is an essential component of preparative regimens for hematopoietic stem cell transplantation, playing a critical role in eradicating malignant cells and suppressing the immune system to enhance the success rate of bone marrow transplants and similar procedures [1–4]. The key to a successful TBI lies in achieving a uniform radiation dose across the entire body. Currently, the bilateral beam technique, among others, is predominantly employed for TBI delivery [5]. To use the bilateral beam technique, the gantry is rotated to 90° (or 270°), and the collimator is rotated to 315°. The distance between the patient and the radiation source is extended to 400 cm (which means source to axis distance (SAD) is 400 cm) to ensure that the field covers the entire patient. Due to the distinct methodology from traditional radiation therapy (RT), the planning process for TBI also differs, involving the division of the human body into sections to calculate the radiation dose for each part. The current TBI dose calculation protocol in our institution follows the formulas outlined in the literature [1, 6] and divides the human body into 13 sections to assess radiation dose. This protocol adapts values for tissue maximum ratio (TMR), off axis ratio (OAR), scatter factors (i.e., S_c and S_p) based on the effective field sizes and uses the compensators to deliver uniform dose to entire body. Following the first fraction, in vivo measurements at 13 locations are conducted to verify the appropriateness of the calculated dose and the number of compensators. Adjustments to the compensators are made based on the results of the in vivo measurements during the first session to ensure subsequent fractions more closely match the prescribed dose. The established practice of in vivo OSLD measurements is well-documented in previous research, offering a solid foundation for this approach [4, 6]. This ensures that a dose close to the prescribed amount is delivered to each section by calculating the number of compensators needed without acquiring any computed tomography (CT) images from the CT simulator. Since the dose calculation based on CT images is not performed using the conventional treatment planning system, in vivo measurements must be conducted during the first treatment to ensure the accuracy of the dose calculation and the number of compensators.

Numerous studies have been conducted to ensure accurate dose measurements in TBI [7–15]. These studies have utilized various dosimeters, such as metal–oxide–semiconductor field-effect transistor (MOSFET), optically stimulated luminescence dosimeter (OSLD), semiconductor diodes, thermoluminescence dosimeters (TLD), and glass dosimeters, to measure surface doses. The measured surface doses were then employed to evaluate midline doses. Typically, midline dose estimation involved summing the dose values at the beam entrance and exit surfaces and applying a correction factor or using methods such as TMR or specific algorithms to derive the midline dose. Additionally, these measurement methods demonstrated uncertainties below 5%, making them suitable for use in TBI, where the goal is to deliver the uniform dose to entire body within ± 10% of prescribed dose [2, 5].

However, discrepancies between calculated dose and in vivo measurements from 2018 to 2022 have revealed uncertainties at the time of the first fraction, demonstrating a single correction factor is insufficient which assumes a linear relationship between variables. Machine learning models demonstrate powerful predictive performance, particularly when there are a wide variety of input features and a sufficient number of samples, and nonlinear relationships between features [16, 17]. This ability makes machine learning models particularly suited for dose prediction in TBI, where patient-specific factors and treatment variables can significantly influence outcomes. By leveraging machine learning, we aim to develop a model that surpasses the predictive capabilities of traditional methods, providing more precise dose estimations and the number of compensators.

This study seeks to identify the most suitable machine learning model for our site's patient data (96 patients, each with 13 dose measurement locations) who undergone TBI with the goal of predicting the dose of each organ before the first fraction using in vivo measured doses as the target. Furthermore, by using a well-trained model, we aim to determine the optimal number of compensators, thereby establishing a more accurate TBI calculation system that better aligns with the prescribed dose.

Method and materials

Conventional method to calculate MUs and the number of compensators

In our institution, TBI treatments utilize bilateral beams, a commonly used technique that aims to deliver a uniform dose distribution to the patient's body. The treatment planning process starts by designating the hip as the reference organ. Based on the hip thickness and patient height, the photon energy (6 MV or 15 MV) and treatment posture (knee-bent or extended) are determined to ensure proper coverage (Fig. 1).

Initially, the monitor unit (MU) needed to deliver the prescribed dose to the reference organ is calculated as:

$$MU = D_p/(TMR \cdot S_c \cdot S_p \cdot SDDF \cdot TF \cdot OAR), \quad (1)$$

where D_p is prescribed dose in cGy, TMR is tissue maximum ratio at depth of the reference organ (half of thickness), S_c is the collimator scatter factor, S_p is the phantom

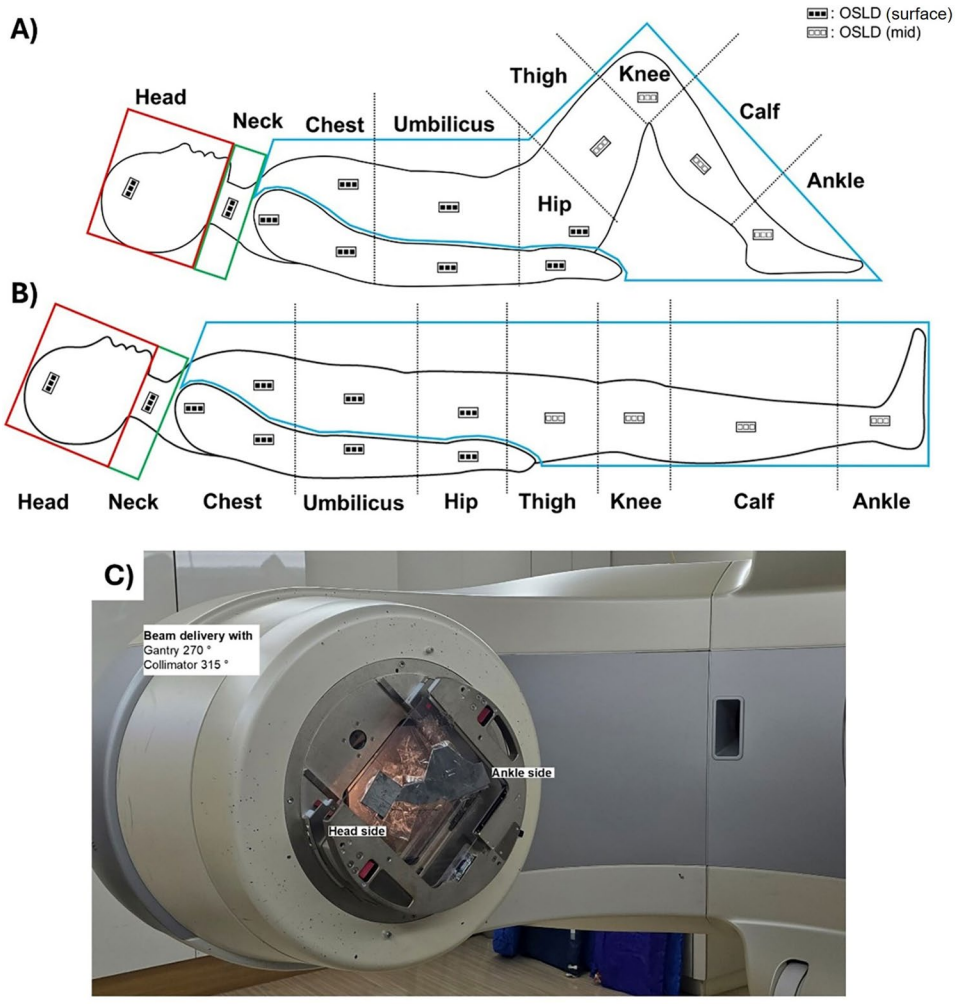

Fig. 1 The patient's posture and the location of OSLDs when using bilateral beam. (**A**) The posture with the knees bent, (**B**) The posture with the knees fully extended, (**C**) The compensators mounted on the LINAC

scatter factor, SADF is source to axis distance factor, TF is transmission factor by the beam spoiler and compensators and OAR is the off-axis ratio of the organ. The relevant factors are detailed in Tables S1, S2, and S3 in supplementary document. Using the calculated MU in Eq. (1), the dose to other organs is calculated as Eq. (2):

$$D_c = MU \cdot TMR \cdot S_c \cdot S_p \cdot SADF \cdot TF \cdot OAR, \quad (2)$$

where D_c is calculated dose by conventional protocol of this institution. The number of compensators (N_c) required for each organ is determined to deliver prescribed dose and to ensure a uniform distribution of radiation across the entire body. They are often adjusted based on the clinical experience. Upon the initiation of the first radiation session, OSLDs are utilized to measure the dose, D_m, received by various organs. When D_m has large discrepancy (exceeding $\pm 10\%$) compared to D_p, further adjusting the compensator can be considered. This adjustment process allows for a refined, patient-specific approach to TBI, where medical physicist may modify the compensators for certain organs based on clinical experience and the data collected from OSLD measurements. To compare the conventional method with the machine learning models, the whole patient's data were assessed using the mean absolute percentage error (MAPE) and by the mean absolute error (MAE).

OSLDs for in vivo measurements

For the OSLD measurement, the InLight nanoDots (Landauer, Inc., Glenwood, IL) were used. Following procedures outlined in prior literature, we replicated the preparation of OSLDs using identical methods [6]. This involved subjecting the dosimeters to a pre-irradiation process, exposing them to doses exceeding 5 kGy from a ^{60}Co gamma ray source to ensure comprehensive saturation of deep electron and hole traps [18]. Subsequently, a bleaching process spanning over 4 h was implemented

to diminish the signal to levels below the residual signal. Those fully filled deep electron and hole traps and optimized bleaching time made the uncertainty of OSLDs less than 3% with TBI beam configurations [6, 18]. The R^2 of calibration curve was 0.99 within calibration range (20–500 cGy) which is sufficient range to cover the prescribed dose per fraction of the TBI. Through adherence to these established procedures, we sought to replicate the stability and accuracy demonstrated in previous studies.

Two sets of OSLDs at the beam entrance and exit surface are used for each organ to determine midline dose (Fig. 1) and each set contains three OSLDs to use the averaged value. The midline dose is determined as the sum of entrance and exit dose with correction factors by previous literature [6, 18]. The organs to measure the midline doses are head, neck, shoulder, chest, umbilicus, hip, thigh, knee, and ankle. The chest, umbilicus and hip are measured with and without hand or arm.

Patient data collection

This retrospective study analyzed patient data collected from our institution, focusing on individuals who underwent TBI between 2018 and 2022. The protocol received Institutional Review Board (IRB) approval, ensuring compliance with ethical standards and the protection of patient confidentiality. The study encompassed a total of 96 patients, with data including demographics, treatment specifics, and in vivo dose measurements extracted from medical records. The fractionation schemes followed our institutional protocol. Specifically, 21, 9, 3, and 63 patients delivered 1, 2, 3, and 4 fractions, respectively. The prescribed dose per fraction was 200 cGy for 26 patients, 250 cGy for 1 patient, and 300 cGy for 69 patients. Each patient has 13 organ sites that had been irradiated and measured. Therefore, 1248 samples were used to train and test the machine learning models.

Development of machine learning model

For in vivo dose prediction in TBI, we developed a machine learning model. The entire patient dataset (96 patients including 1248 samples) was divided into a training set (70%, 67 patients including 871 samples) and a test set (30%, 29 patients including 377 samples. The input features for the model training were the patients' gender, age, weight, height, the photon energy used, MU, organ name, D_p, D_c, and N_c with the target being the D_m. This approach assumed that the D_m represents the true value of the radiation dose in this study.

To identify the most suitable machine learning model for our data, we conducted a comparative analysis of model performance, utilizing the MAPE between D_m and predicted dose by machine learning models (D_{ML}). The models considered in this evaluation included random forest regressor (RF) [19], extreme gradient boost (XGBoost) [20], gradient boost regressor (GBR) [21] and light gradient boost machine (LightGBM) [22]. Those models demonstrated robust, consistent, and superior performance (lower MAPE) compared to other machine learning models. Following the model selection process, hyperparameter tuning was undertaken to further refine the chosen model's performance. To validate the necessity of using machine learning algorithms, a simple multiple linear regression analysis was also conducted for each treatment site using the same input features (without organ name). This allowed for a direct comparison between linear statistical modeling and the non-linear machine learning approaches. We calculated the MAPE between D_m and predicted dose by multiple linear regression model (D_L).

Moreover, to understand the dependency of the model on the training data and to ensure its robustness, we employed a k-fold cross-validation technique, specifically applying a 10-folds. This method not only provided insights into the model's stability across different subsets of the training data but also helped in mitigating the risk of overfitting, ensuring that the final model is both reliable and generalizable across various patient data. Through meticulous training, feature selection, and rigorous validation, this approach aims to enhance the accuracy of dose prediction in TBI, paving the way for more accurate and personalized treatment plans.

The selected and trained machine learning model will be evaluated by comparing MAPE between D_m and D_{ML} using the test set. Through this comparison, the performance and accuracy of the final model is comprehensively understood and validated in terms of predicting the dose. Subsequently, paired t-tests were performed to assess the statistical significance of the difference between D_c and D_{ML}, and between D_L and D_{ML}.

The optimization of the number of compensators

Utilizing the developed machine learning model, we were able to predict in vivo doses using patient's information and the number of the compensator prior to the irradiation. This predictive capability facilitated a more precise approach to delivering radiation doses that close to the prescribed dose (D_p) than conventional method. To minimize the discrepancy between D_p and D_{ML} for each organ, the number of compensators was adjusted. Here, D_{ML} represents the predicted dose with the N_c. Through an iterative optimization process using machine learning model, we determined the optimized number of compensators (N_{op}) that yielded the minimal dose difference. The resulting dose predicted with N_{op}, is denoted as D_{op}. We compared N_c with N_{op}, and evaluated the MAPEs between D_p and D_{op} for various organs.

Results

Conventional method

As seen from Fig. S1 in supplementary document, measured dose values at the chest without arm are in the range of 250–300 cGy, which is lower than the prescription dose of 300 cGy. This intentional reduction is attributed to an empirical adjustment derived from clinical observations. Empirical evidence indicated that the measured dose in this region tended to be slightly higher than the calculated dose due to calculation uncertainties. To compensate for this potential overdose and strictly ensure that the lung dose does not exceed 300 cGy, additional compensators were added in the treatment planning process. Consequently, this conservative approach resulted in the measured dose being lower than the prescribed dose. Regarding the calculation accuracy (comparing between D_c and D_m), the overall MAPEs across all organs was 4.01%. The largest error was for head, 8.69% while the umbilicus without arm showed the smallest difference as 2.74%. On the other hand, the agreement between the D_p and the D_m implies the successfulness of dose planning using the conventional method, showed an overall MAPE of 3.65%. In this comparison, the largest difference was found in the chest without arm, 6.01% and the smallest difference was in the umbilicus without arm, 2.61%. The MAPEs between D_p and D_c, and between D_m and D_c, and between D_p and D_m of each organ are shown in Fig. S2.

Model performance

All the machine learning models outperformed the conventional method and multiple linear regression in terms of MAPE and showed significant difference with p-value < 0.05. The estimated doses by conventional method, linear regression model, machine learning model and measured dose of test data set are shown in Table 1; Fig. 2(A). The figure shows that in most of cases the predicted doses by machine learning models were closer to the measured dose. During the training phase, there was no significant difference in the learning time across four models.

The MAPEs between the D_m and D_{ML} by the machine learning models were 2.52, 2.51, 2.67, and 2.67% for GBR, LightGBM, XGBoost, and RF respectively. To ensure that the predictions of the models were not dependent on the choice of training data, the models underwent a k-fold cross-validation process with 10 folds. The GBR and LightGBM showed the best performance in predicting the doses.

Optimization of compensator

The MAPEs between D_p and D_{op} for the test data set ($N = 377$) are presented in Fig. 2(B) and Table 2. Among the evaluated models, the GBR model achieved the lowest MAPE of 1.69%, which is selected as the best model. Additionally, Table 2 summarizes the changes in the number of compensators following the optimization process.

During the optimization process, some of the compensators were not adjusted if their predicted dose is already close to the prescribed dose. Regarding the sign convention for the compensator difference in Table 2, a positive value indicates an excess of initially calculated compensators, necessitating a reduction. Conversely, a negative value indicates an insufficiency, requiring the addition of compensators. The Fig. 3 illustrates D_{ML} with initial compensator and D_{op} with optimized compensator, showing that the optimized compensators can offer close

Table 1 The MAPEs (%) between D_m and D_c (Conv.); D_m and D_L (Linear regression); and D_m and D_{ML} (Machine learning models) from the test set ($N = 377$). The lower error means the more accurate to predict measured dose

Organ	Conv.	Linear Regression	Machine learning models			
			GBR	LightGBM	XGBoost	RF
Overall	4.01	3.25	2.52	2.51	2.67	2.67
Head	8.69	3.37	2.67	2.63	2.76	3.00
Neck	3.87	2.59	2.51	2.49	2.79	3.10
Shoulder	3.82	2.61	2.20	2.00	2.31	2.28
Chest without arm	3.65	4.49	2.56	2.38	2.63	2.58
Chest with arm	3.10	3.06	2.54	2.41	2.91	2.69
Umbilicus without arm	2.74	3.21	2.19	2.37	2.06	2.28
Umbilicus with arm	4.82	3.28	2.36	2.46	2.40	2.29
Hip without hand	4.12	3.09	2.36	2.45	2.51	2.37
Hip with hand	3.96	4.21	2.95	3.00	3.34	3.26
Thigh	4.39	3.21	2.79	2.69	3.00	2.94
Knee	3.04	3.38	2.69	2.73	2.86	2.70
Calf	3.18	2.95	2.44	2.61	2.46	2.43
Ankle	3.00	2.75	2.58	2.42	2.72	2.82

MAPE, Mean absolute percentage error; Conv, Conventional method used in our institution; GBR, Gradient boost regressor; LightGBM, Light gradient boost machine; XGBoost, Extreme gradient boost; RF, Random forest regressor

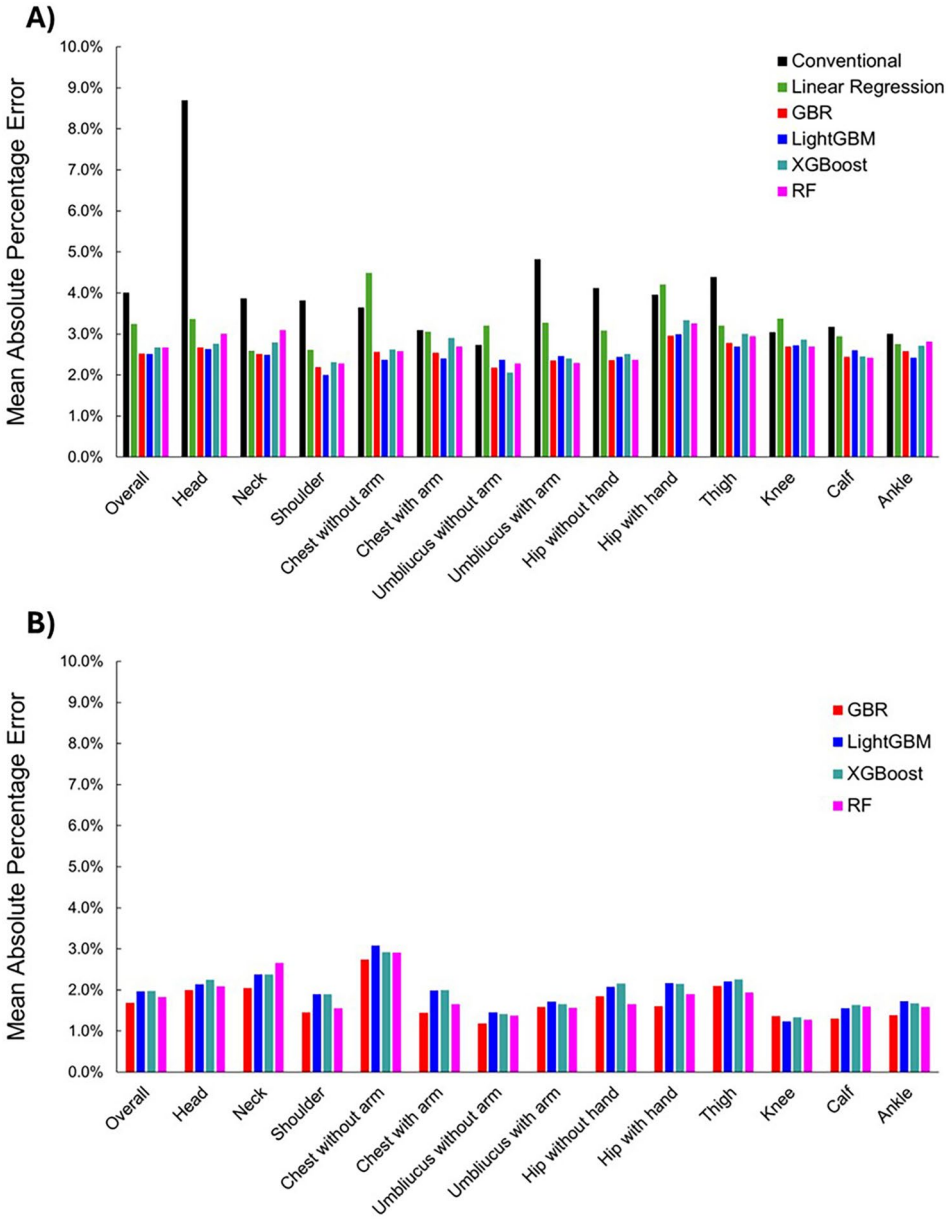

Fig. 2 The error comparison from test set ($N = 377$). (**A**) The MAPE between measured dose (D_m), and calculated dose (D_c) denoted as 'Conventional', and between D_m and predicted dose (D_L and D_{ML}). (**B**) The MAPE between D_p (prescribed dose) and D_{op} (predicted dose with optimized compensators). 'Conventional' represents the MAPEs between D_m and D_c by conventional method in our institution. GBR, Gradient boost regressor; LightGBM, Light gradient boost machine; XGBoost, Extreme gradient boost; RF, Random forest regressor

predicted doses to D_p. We specifically selected the head and neck regions among 13 organs for detailed analysis. The head was chosen due to its largest discrepancy with conventional method, while the neck was selected for demonstrating the greatest variation between the initial and optimized number of compensators. In the head region, which typically shows a tendency for dose overestimation in conventional TBI planning (Fig. S1), the optimization process effectively corrected this deviation. As a result, the average dose was adjusted to align closely with the prescription dose from the average of D_{ML}, 291.71 cGy to the average of D_{op}, 299.99 cGy. Conversely, the neck region presented a persistent challenge. While the optimization process brought the dose closer to the prescription dose, reducing the average D_{ML}, of 310.45 cGy to a D_{op} of 307.26 cGy, the results indicated that additional compensators are still required to fully correct the dose discrepancies in this region.

Table 2 MAPEs (%) between prescription dose (D_p) and predicted dose with optimized compensators (D_{op}), and changes of the number of compensators

Organ	Machine learning models				Number of compensators		
	GBR	LightGBM	XGBoost	RF	N_c	N_{op}	Difference ($N_c - N_{op}$)
Overall	1.69	1.96	1.97	1.83	2.55	2.48	0.07
Head	2.00	2.14	2.24	2.09	4.79	4.34	0.45
Neck	2.05	2.38	2.38	2.66	5.86	6.52	-0.66
Shoulder	1.45	1.89	1.90	1.56	0.28	0.66	-0.38
Chest without arm	2.74	3.08	2.92	2.92	3.03	2.00	1.03
Chest with arm	1.45	1.99	2.00	1.65	0.14	0.17	-0.03
Umbilicus without arm	1.18	1.46	1.42	1.37	2.76	2.79	-0.03
Umbilicus with arm	1.59	1.72	1.66	1.56	0.00	0.34	-0.34
Hip without hand	1.85	2.08	2.16	1.66	2.10	1.52	0.58
Hip with hand	1.61	2.17	2.14	1.90	0.00	0.34	-0.34
Thigh	2.10	2.21	2.26	1.94	2.86	2.21	0.65
Knee	1.37	1.24	1.33	1.28	3.21	3.03	0.18
Calf	1.30	1.56	1.64	1.59	3.38	3.10	0.28
Ankle	1.38	1.72	1.68	1.58	4.72	5.21	-0.49

N_c represents initial number of compensators, while N_{op} is optimized number of compensators. N_c or N_{op} for single patient is an integer, as the N_c and N_{op} listed in this table are not. This is because they are averaged for 29 patients

Discussions

In this study, a machine learning approach was used to enhance the conventional method previously used for TBI dose planning at our institution. The results showed that head region has the largest discrepancy using the conventional method for the dose planning. Through machine learning approach, we were able to significantly address these discrepancies. Additionally, the optimization process further reduced discrepancies, allowing for dose planning that more closely approximates the prescription dose before the first beam delivery. The dose predictions made by the machine learning model were more accurate across all regions compared to the conventional method, particularly in the head region, while regions such as the chest, knee, and ankle showed relatively less improvement.

In this study, we adopted a two-step approach, dose prediction followed by optimization, rather than directly predicting the number of compensators. This strategy was chosen to ensure clinical flexibility and safety. Direct prediction of compensators can act as a black box without verification, making it difficult to verify the dosimetric status prior to treatment. By explicitly predicting the in vivo dose first, clinicians can assess the patient's condition and apply specific constraints, such as limiting doses to organ at risk or adjusting doses based on individual anatomy. This transparency allows for a rigorous quality assurance process and enables patient-specific dose modulation.

A specific observation from our optimization results reinforces the necessity of this flexible approach. As indicated in Table 2, the chest without arm region exhibited the largest adjustment in the number of compensators (a mean change of 1.03). This significant variation stems from the experimental design, where the prescribed dose (D_p) was standardized across all anatomical regions for consistent statistical evaluation. In clinical practice, however, the chest dose is typically restricted to spare the lungs, which are critical OAR. Consequently, because the model was tasked with achieving the standard therapeutic dose rather than the clinically reduced lung dose, it interpreted the conventional setup as under-dosed and predicted a substantial adjustment to the compensators. This can be seamlessly addressed by inputting the patient-specific, dose-reduced prescription for the chest region into the optimization model, ensuring appropriate lung sparing while maintaining prediction accuracy.

This enhancement in dose prediction capability facilitated the execution of the optimization process which is instrumental in refining the treatment protocol for TBI, ensuring that the optimized radiation dose (D_{op}) delivered across the target area is as uniform as possible and closely matches the prescribed dose. The ability to predict and adjust the number of compensators before the first irradiation represents a significant advancement in personalized patient care, as it allows for a more accurate and tailored approach to radiation therapy. By harnessing the power of machine learning for dose prediction, this method provides a more sophisticated and data-driven strategy for compensator quantity optimization, highlighting the potential of computational techniques in enhancing the efficacy and accuracy of TBI treatments. This approach represents a significant paradigm shift in TBI treatment planning, moving from traditional empirical estimation to data-driven precise prediction. While conventional TBI has historically relied on manual calculations and generalized assumptions, our approach introduces a data-driven framework that explicitly accounts

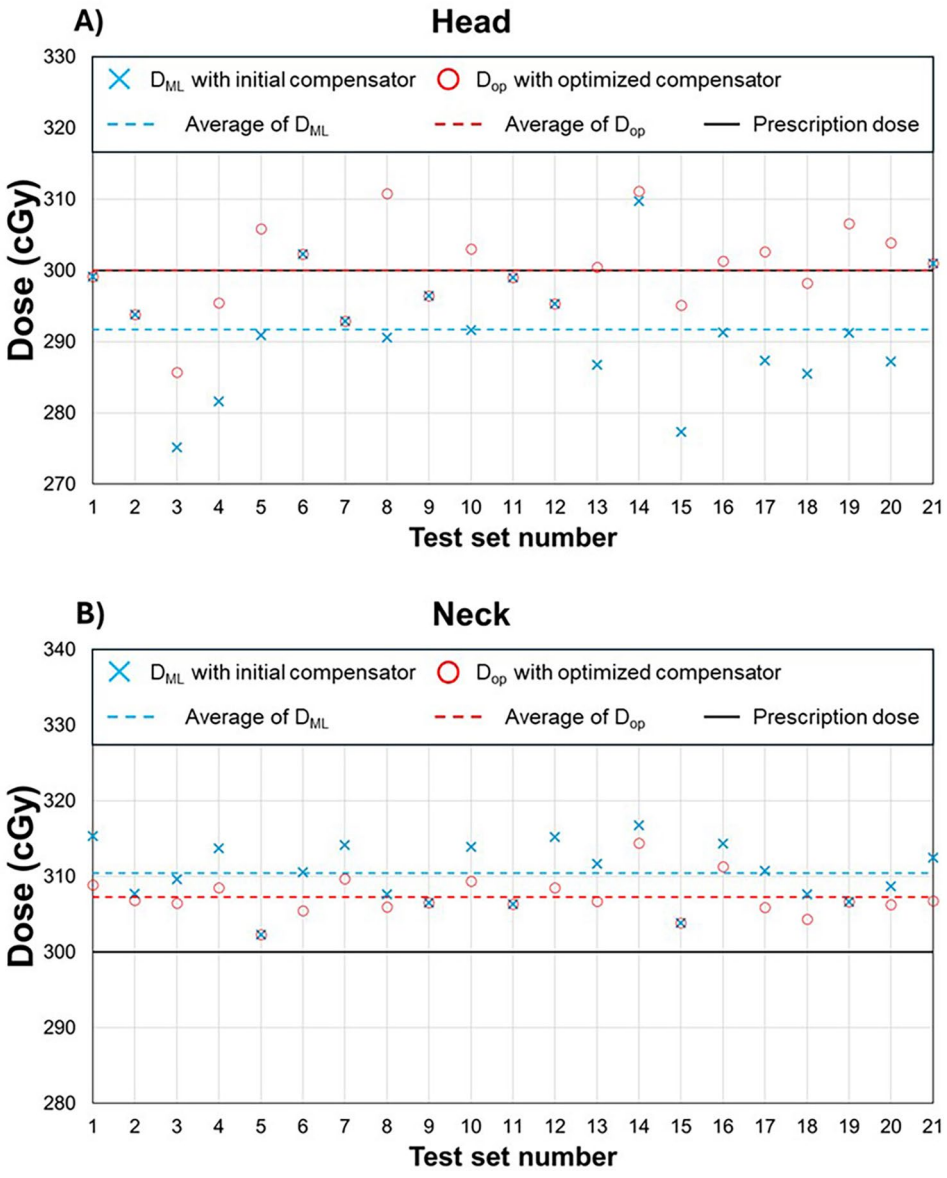

Fig. 3 Comparison of predicted doses before and after the optimization process. The data points were selected from the test set where the prescription doses were 300 cGy. The number of compensators was optimized with gradient boost regressor (GBR) model, which showed the best performance in predicting dose. D_{ML}, prediction dose with the initial number of compensators; D_{op}, prediction dose with the optimized number of compensators

for individual patient heterogeneity. By successfully integrating machine learning into this conventional framework, our study demonstrates that high-level dosimetric accuracy and personalized optimization can be achieved without the need for fundamental changes to the beam delivery system. Furthermore, a recent study on customized aluminum compensators demonstrated that material advancements could improve dose accuracy and workflow efficiency [23]. Inspired by such findings, our future work will aim to integrate our machine learning optimization model with advanced compensator materials like aluminum. We anticipate that combining our algorithmic precision with superior hardware materials will lead to the ultimate level of accuracy and efficiency in TBI treatments.

However, as the proposed machine learning approach in this study is based on a single institutional model, its applicability to other institutions may require further investigations. Another limitation of this study is that the dose measured by OSLDs does not account for the tissue lateral effect, which increases with the patient's thickness. This is because, while the variation in lateral tissue effect with phantom thickness has been identified in previous studies, the impact of thickness changes in irregular shapes on the lateral tissue effect has not been studied under the beam configuration of this institution.

Therefore, in cases where the patient has a greater thickness, the maximum dose that the patient could receive may be up to approximately 10% higher than the midline dose determined by the OSLDs.

Traditional calculation methods based on the effective field size showed different patterns depending on the presence of the arms underestimating doses in the chest area when arms were absent and in the umbilicus when arms were present. This phenomenon is likely due to the irregular shape of the target when viewed laterally in the beam's eye view, compounded by the generally thicker arms in the chest area. The future work will involve verifying how closely the dose values predicted by the optimization process matches with actual measurements.

Beyond TBI, the proposed machine learning approach could be extended to other treatment situations where routine dose measurement reveals the discrepancies between planned and delivered dose. Examples include total skin electron beam therapy (TSEBT), stereotactic body radiation therapy (SBRT) that employ dose verification with the dose measurement. In these settings, the core principle remains identical to the present study, a model trained on measured dose as the target while planning parameters as input features. We anticipate that such machine learning aided corrections will become increasingly valuable as treatment situations demand tighter tolerance on dose delivery.

Conclusion

The machine learning approach was successfully trained to accurately predict in vivo dose measurements, showing potential to enhance conventional methods. Specifically, the GBR model achieved a prediction error (MAPE between D_m and D_{ML}) of 2.52%, a significant improvement over the conventional calculation error (MAPE between D_m and D_c) of 4.01%. Based on this improved accuracy, the subsequent optimization process demonstrated the capability to generate treatment plans that closely approximate the prescribed dose. The optimization process successfully converged to a solution with a theoretical agreement (MAPE between D_p and D_{op}) of 1.69%. This result indicates that the proposed machine learning approach has the potential to supplement conventional methods by providing more refined treatment strategies.

Abbreviations

CT	Computed tomography
D_c	Calculated dose
D_L	Predicted dose by linear regression
D_m	Measured dose
D_{ML}	Predicted dose by the machine learning model
D_{op}	Optimized dose by the machine learning model
D_p	Prescribed dose
GBR	Gradient boost regressor
IRB	Institutional review board
LightGBM	Light gradient boost machine
MAE	Mean absolute error
MAPE	Mean absolute error
MAPE	Mean absolute percentage error
MOSFET	Metal oxide semiconductor field effect transistor
MU	Monitor unit
N_c	Calculated number of compensators
OAR	Off axis ratio
OSLD	Optically stimulated luminescence dosimeter
RF	Random forest
RT	Radiation therapy
SAD	Source to axis distance
SADF	Source to axis distance factor
SBRT	Stereotactic body radiation therapy
S_c	Collimator scatter factor
S_p	Phantom scatter factor
TBI	Total body irradiation
TF	Transmission factor
TLD	Thermoluminescence dosimeter
TMR	Tissue maximum ratio
TSEBT	Total skin electron beam therapy
XGBoost	Extreme gradient boost

Supplementary Information

The online version contains supplementary material available at https://doi.org/10.1186/s13014-026-02829-6.

Supplementary Material 1

Acknowledgements

The authors thank In-Ho Lee (Ph.D., Korea Research Institute of Standards and Science) for advice on the design of machine learning models and analysis.

Author contributions

SJ and JIK supervised the project, and designed the concept and the experiment method of the research. SK, JS, HJ, CHC, JMP, JHL, JHC, and HCK supported on data collection and the characterization of the sample. SL and SJ performed the experiment and data analysis. SL wrote the paper and prepared Figures and Tables. SJ revised the manuscript. All authors have reviewed the final manuscript.

Funding

This study was funded by National Research Council of Science & Technology (NST), Grant Number: CAP22041-100 and the Korea Research Institute of Standards and Science (KRISS), Grant Number: GP2026-0008-02.

Data availability

The authors confirm that the data supporting the findings of this study are available within the article and its supplementary materials.

Declarations

Ethics approval and consent to participate

All procedures performed in study involving human participants were in accordance with the ethical standards of the institutional review board (IRB approval No. H-2405-047-1535) and with the 1964 Helsinki declaration and its later amendments or comparable ethical standards. Informed written consent was obtained from all individual patients included in this study.

Consent for publication

Not applicable.

Competing interests

The authors declare no competing interests.

Author details

[1]Department of Radiation Oncology, Yonsei Cancer Center, Yonsei University College of Medicine, Seoul, Republic of Korea
[2]Department of Radiation Oncology, Seoul National University Hospital, Seoul, Republic of Korea

[3]Institute of Radiation Medicine, Seoul National University Medical Research Center, Seoul, Republic of Korea
[4]Biomedical Research Institute, Seoul National University Hospital, Seoul, Republic of Korea
[5]Department of Radiation Oncology, Seoul National University, Seoul, Republic of Korea
[6]Ionizing Radiation Group, Division of Biomedical Metrology, Korea Research Institute of Standards and Science, Daejeon 34113, Republic of Korea

Received: 21 June 2024 / Accepted: 13 March 2026
Published online: 11 April 2026

References

1. Khan FM, Gibbons JP. Khan's the physics of radiation therapy. Lippincott Williams & Wilkins; 2014.
2. Dyk JV, et al. The physical aspects of total and half body photon irradiation. Am Assoc Phys Med. 1986.
3. Park J, et al. Effects of total body irradiation-based conditioning on allogeneic stem cell transplantation for pediatric acute leukemia: a single-institution study. Radiation Oncol J. 2014;32(3):198.
4. Park S-Y, et al. Total body irradiation with a compensator fabricated using a 3D optical scanner and a 3D printer. Phys Med Biol. 2017;62(9):3735.
5. Khan FM, et al. Basic data for dosage calculation and compensation. Int J Radiation Oncology* Biology* Phys. 1980;6(6):745–51.
6. Choi CH, et al. Prediction of midline dose from entrance and exit dose using OSLD measurements for Total body irradiation. J Radiation Prot Res. 2017;42(2):77–82.
7. Scalchi P, Francescon P. Calibration of a MOSFET detection system for 6-MV in vivo dosimetry. Int J Radiation Oncology* Biology* Phys. 1998;40(4):987–93.
8. Ribas M, et al. Midplane dose determination during total body irradiation using in vivo dosimetry. Radiother Oncol. 1998;49(1):91–8.
9. Mangili P, et al. In-vivo dosimetry by diode semiconductors in combination with portal films during TBI: reporting a 5-year clinical experience. Radiother Oncol. 1999;52(3):269–76.
10. Palkoskova P, et al. vivo thermoluminescence dosimetry for total body irradiation. Radiat Prot Dosimetry. 2002;101(1–4):597–600.
11. Bloemen-van Gurp EJ, et al. Total body irradiation, toward optimal individual delivery: dose evaluation with metal oxide field effect transistors, thermoluminescence detectors, and a treatment planning system. Int J Radiation Oncology* Biology* Phys. 2007;69(4):1297–304.
12. Ramm U, et al. In vivo dosimetry with semiconducting diodes for dose verification in total-body irradiation. Strahlenther Onkol. 2008;184(7):376.
13. Rah J-E, et al. Clinical application of glass dosimeter for in vivo dose measurements of total body irradiation treatment technique. Radiat Meas. 2011;46(1):40–5.
14. Satory P. Calculation of midplane dose for total body irradiation from entrance and exit dose MOSFET measurements. Australasian Phys Eng Sci Med. 2012;35:101–4.
15. Akino Y, McMullen KP, Das IJ. Patterns of patient specific dosimetry in total body irradiation. Med Phys. 2013;40(4):041719.
16. Field M, et al. Machine learning applications in radiation oncology. Phys Imaging Radiation Oncol. 2021;19:13–24.
17. Kang J, et al. Machine learning approaches for predicting radiation therapy outcomes: a clinician's perspective. Int J Radiation Oncology* Biology* Phys. 2015;93(5):1127–35.
18. Park S-Y, et al. Sensitivity and stability of optically stimulated luminescence dosimeters with filled deep electron/hole traps under pre-irradiation and bleaching conditions. Physica Med. 2017;38:81–7.
19. Ho TK. Random decision forests. in Proceedings of 3rd international conference on document analysis and recognition. 1995. IEEE.
20. Chen T, Guestrin C. Xgboost: A scalable tree boosting system. in Proceedings of the 22nd acm sigkdd international conference on knowledge discovery and data mining. 2016.
21. Friedman JH. Greedy function approximation: a gradient boosting machine. Ann statist. 2001: 1189–1232.
22. Ke G et al. Lightgbm: A highly efficient gradient boosting decision tree. Adv Neural Inf Proc Syst. 2017;30.
23. Naessige M, et al. A customizable aluminum compensator system for total body irradiation. J Appl Clin Med Phys. 2021;22(10):36–44.

Publisher's note